ISBN: 978-3-95450-262-2 ISSN: 2673-5350 doi: 10.18429/JACoW-IBIC2025-MOPCO19

LARGE DYNAMIC RANGE BEAM INTENSITY MEASUREMENT FOR BOTH H^0 AND PROTON BEAMS IN INJECTION UPGRADE OF CSNS-II*

W. L. Huang†, R. Y. Qiu, X. J. Nie, F. Li, L. Zeng, R. J. Yang, Z. H. Xu
Institute of High Energy Physics, Chinese Academy of Sciences, Beijing, China
Spallation Neutron Source Science Center, Dongguan, China

Abstract

China Spallation Neutron Source (CSNS) upgrade project (CSNS-II) started in 2024. As the first important task, the injection section will be redesigned and a lot of beam instruments will be installed along the injection to I-Dump beam line. The H^0 beam intensity at the downstream of the stripping foils is several microampere during the normal operation, while the proton beam intensity at the I-dump may be over 80 mA during the commissioning of linac and RCS. A corresponding design of the ACCT sensor and electronics is introduced in this paper. There are two nanocrystalline cores in H0CT, providing two different turns ratio for the large dynamic range beam intensity measurement. The gain of the electronics is switchable in two ranges. The INDCT is equipped with only one core and the electronics design is aiming to a high SNR for the injected proton beam power evaluation. Tests in the lab showed a good linearity of the H0CT and INDCT sensors with the electronics. Beam commissioning of the injection section is planned in October of 2025.

INTRODUCTION

As explained in Ref. [1], the H- charge exchange injection technique is adopted to overcome the intensity limitation of the beam emittance increase with the number of injected turns and high losses at the septum. Thus, the multi-turn charge-exchange injection in spallation neutron sources is very common and proved to be effective. In CSNS-II, the injection energy of H^- beam changes from 80 MeV to 300 MeV, beam intensity from 15 mA to 50 mA (or 80 mA) and the maximum pulse width from 550 μs to 650 μs [2]. Thus the injection instruments layout has been redesigned last year [3], including the new chicane and many beam instruments for diagnostics, which consists of two current transformers (H0CT and INDCT), a fluorescent screen (INDVS), 3 multiwire profile monitors (INMWS01, INMWS02 and INDMWS01), an electron collector (INCOL), 8 beam loss monitors and two beam position monitors, as shown in Fig. 1.

The new H0CT has larger inner diameter (120 mm) and aims to evaluate the stripping efficiency and the foil aging, the same as that in CSNS [4]. It measures the ultra-low intensity of H^0, which are not stripped completely by the 1st foil but totally stripped charge changing to H^+ and delivered to the IN-DUMP. While the INDCT has an inner diameter of 160 mm, aiming to measure the proton beam intensity to the INDUMP during the commissioning of the injection zone and the linac. Meanwhile the proton beam passes through the H0CT too, because the two CTs is only 1.2 m away. So the BCT in H0CT is a dual-function low noise current monitor and a new two-range electronics was designed for both H0CT and INDCT. Crosscheck is very convenient between the readouts of the two current monitors.

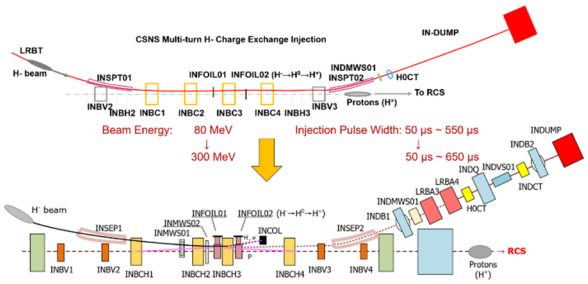

Figure 1: Different layout of the injection zone in CSNS and CSNS-II.

SENSOR DESIGN AND FABRICATION

As in Ref. [5], the classical transformer circuit is depicted in Fig. 2. Current in any N turn winding k produces magnetic flux in the core of magnitude $\Phi_k = L_k \cdot i_k / N_k$. The voltage appearing across each winding is proportional to the time rate change of the total flux Φ_T. The beam is seen as 1 turn wire, then we find

$$\frac{i_s}{i_{beam}} = \frac{1}{N_s} \cdot \left(1 + \frac{R_s}{N_s^2 \cdot R_{beam}}\right)^{-1}. \quad (1)$$

For $R_{beam} \gg R_s$, the familiar approximate result, $i_s = i_{beam}/N_s$, is obtained. The secondary current is very closely equal to $1 / N_s$ times the beam current. The sensor response to a bunch pulse is characterized with a risetime and droop. The droop time is figured as L_s / R, indicating that a large L_s and a small R will lead to a slow droop.

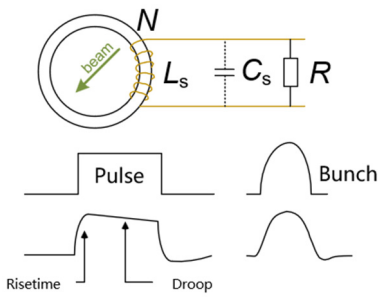

Figure 2: Equivalent circuit and pulse response of a classical current transformer [6].

* This work is supported in part by National Key R&D Program of China under Contracts No. 2023YFE0105700, and National Natural Science Fund (No. 12275294).
† huangwei@ihep.ac.cn

ISBN: 978-3-95450-262-2 ISSN: 2673-5350 doi: 10.18429/JACoW-IBIC2025-MOPCO19

The macro pulse width of the injected H^- beam is 100 to 650 μs. It requires the risetime of H0CT and INDCT is less than 30 μs, and the droop should be less than 1 %/ms. Thus we choose an iron-based soft magnetic alloy core wound with very thin ribbons (20 μm) in high permeability($\mu_r \approx 80000$), low loss, and nearly zero magnetostriction, to make the 50-turn BCT(ACCT) in H0CT and INDCT, a 20-turn FCT was also installed in H0CT for experiment in frequency domain. Table 1 gives the designed specification and some parameters of H0CT and INDCT.

Table 1. Designed Specification and Some Parameters of H0CT and INDCT

Sensor	H0CT	INDCT
Range	±200 μA ±100 mA	
Core size /mm	ID140OD180H20	ID180OD220H20
Turns	50	50
L_s	290 mH@10 Hz	252 mH@10 Hz

The longitudinal length of H0CT and INDCT is the same as the uninstalled H0CT, 300 mm. The mechanical drawing of the new H0CT (inner diameter 110 mm) is showed in Fig. 3. The double-layer magnetic shielding is made of DT4, a kind of industrial pure iron. There are two lays of copper sheet with a sheet of polymide between them to form a capacitor just over the ceramic ring, which acts as a LP filter for the sensor. The mechanical structure of INDCT is similar to that of H0CT, except that there isn't an FCT core in INDCT.

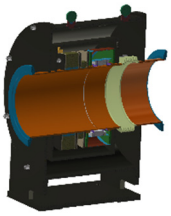

Figure 3: Mechanical drawing of the new H0CT.

There is one winding for intensity calibration of BCTs and triaxial cables are used to transport the sensor signal, the same as those in CSNS. The equivalent circuits of the BCT sensor, the triaxial cable and the electronics is showed in Fig. 4. According to the experience of the uninstalled H0CT of CSNS, the noise was eliminated by grounding the triaxial cable outer shielding at both the sensor side and the electronics side, providing a better SNR.

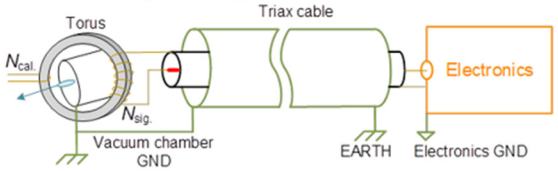

Figure 4: Equivalent circuits of BCTs in H0CT and INDCT [4].

INTERFERENCES AND NOISES

During the commissioning of the power supplies of magnets in injection zone and the RF power sources in adjacent area, big interferences were observed although the beam is off and no calibration is done to the H0CT and INDCT. Figures 5 and 6 show the interferences (25 Hz) from the RF power source of a ferrite-loaded cavity to the H0CT and the INDCT. When we used a function generator to measure the droop of INDCT (100 Hz square wave with an amplitude of 5 mVpp) during the pulsed power supplies for septums were on, the sharp pulsed interference appeared on the output waveform of the electronics, shown in Fig. 7. This made the droop measurement very difficult.

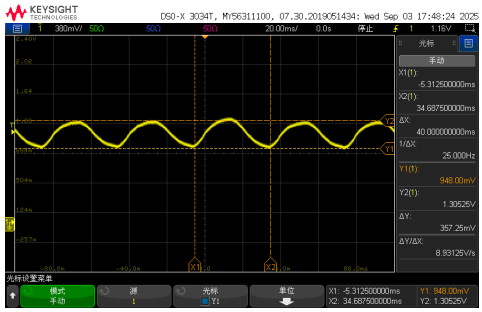

Figure 5: Interferences (25 Hz) from the RF power source of a ferrite-loaded cavity to the H0CT electronics.

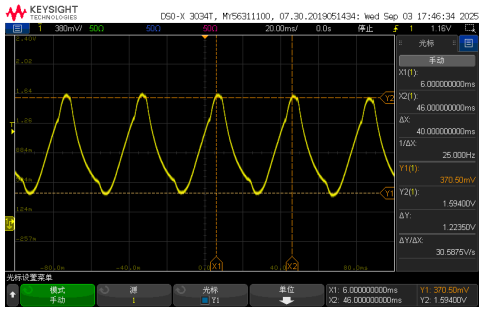

Figure 6: Interferences (25 Hz) from the RF power source of a ferrite-loaded cavity to the INDCT electronics.

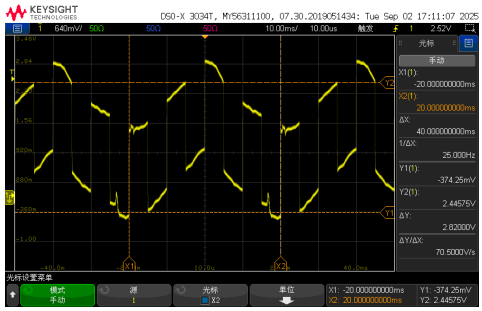

Figure 7: Combined interferences (25 Hz) from the pulsed power supplies of septums and the RF power source of a ferrite-loaded cavity to the INDCT electronics.

We may cancel the noise by the data acquisition system for data readout and post processing algorithm, that is, the sensor signals without beam on are acquired by the electronics and the background data is recorded and stored in the LabVIEW program buffer, when the beam is on, the

ISBN: 978-3-95450-262-2 ISSN: 2673-5350 doi: 10.18429/JACoW-IBIC2025-MOPCO19

front part of the pulse waveform is averaged with the rear part to get the mid value of baseline, then the mid value is added to the stored noise as a constant. This is executed for each bunch. The method of noise elimination and baseline recovering will be tested in the RCS commissioning this September.

CALIBRATIONS OF H0CT AND INDCT

A KEITHLEY6221 DC/AC current source was used to calibrate the BCTs and electronics of H0CT and INDCT, as shown in Fig. 8. The oscilloscope stands for the DAQ. An automatic readout and average algorithm was programmed in LabVIEW and used in BCT calibration.

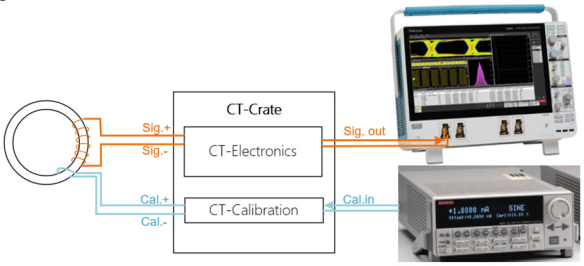

Figure 8: Calibration scheme of the BCTs.

We changed the output current from 10 μA to 200 μA in a step of 10 μA and from 5 mA to 100 mA in a step of 5 mA. The linearity error is within ±0.5 %, and the sensitivity is designed as ±100 mA / ±10 Vout and ±200 μA / ±10 Vout shown in Fig. 9 for H0CT and Fig. 10 for INDCT.

The risetime and droop measurement is done with a KEYSIGHT 33522 function generator and KEYSIGHT DSO X3034T oscilloscope. Table 2 gives the measurement results of BCTs in H0CT and INDCT. It shows that both BCTs in H0CT and INDCT have a rise time of <30 μs and a droop of <1 %/ms with the new electronics.

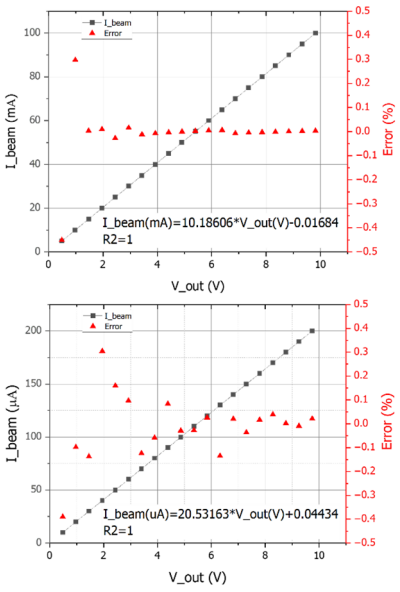

Figure 9: Calibration of the H0CT and electronics.

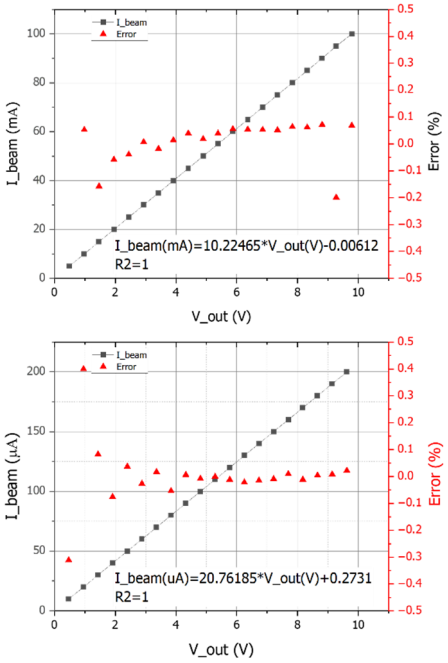

Figure 10: Calibration of the INDCT and electronics.

Table 2. Designed Specification and Some Parameters of BCTs in H0CT and INDCT

Sensor	H0CT	INDCT
Risetime (μs)	24.64	23.91
Drop (% /ms)	0.36	0.89

The two current transformers H0CT and INDCT were installed at the injection region in the accelerator tunnel during this summer maintenance. The DAQ system consists of an NI PXI-6358 card and an NI controller for electronics readout of this large dynamic intensity measurement by changing the range according to the accelerator operation mode. In the electronics, the OPA range is set to ±200 μA as default by the do/i of the PXIe-6358. As long as the of electronics readout exceeds 10 V, the OPA range will be switched to the range of ±100 mA. This will protect both the electronics and the readout system. In the future, the INDCT readout will be included into the machine protection system to indicate the exceeding of beam power bombarding onto the I-Dump.

CONCLUSION

In order to meet the requirement of injection upgrade of CSNS-II, we designed two new current monitors, H0CT and INDCT. For the large dynamic range of stripped $H^0(H^+)$ and proton beam intensity (several microampere to a hundred milliampere), two new sensors were fabricated and a two-range electronics was designed. All the specifications including linearity, risetime and droop were measured in the lab and passed the acceptance. An FFT algorithm of the FCT readout, which comes from Ref. [7] will be tested in the further system commissioning.

ISBN: 978-3-95450-262-2 ISSN: 2673-5350 doi: 10.18429/JACoW-IBIC2025-MOPCO19

REFERENCES

[1] C. Bracco, "Phase Space Painting and H- Stripping Injection", in *Proc. CAS'17*, Erice, Italy, Mar. 2017, pp. 141-149. doi: 10.23730/ CYRSP-2018-005.141

[2] S. Fu and S. Wang, "Operation Status and Upgrade of CSNS", in *Proc. IPAC'19*, Melbourne, Australia, May 2019, pp. 23-27. doi:10.18429/JACoW-IPAC2019-MOZPLM1

[3] M. Y. Huang, S. Wang, and S. Y. Xu, "Performance and Upgrade Considerations for the CSNS Injection", in *Proc. HB'23*, Geneva, Switzerland, Oct. 2023, pp. 326-330. doi:10.18429/JACoW-HB2023-THA1I1

[4] R. Y. Qiu, *et al.* "Development of an H^0CT measurement system at the CSNS injection region", *High Power Laser Part. Beams*, vol. 35, no. 2, p. 024004, 2023. doi: 10.11884/HPLPB202335.220142

[5] R. C. Webber, "Tutorial on beam current monitoring", *AIP Conf. Proc*., vol. 546, no. 1, pp. 83-104, 2000. doi: 10.1063/1.1342580

[6] Peter Fork, Lecture Notes on Beam Instrumentation and Diagnostics, in *JUAS'11*, Archamps, France, Jan.-Mar. 2011.

[7] P. K. Saha *et al.*, "State of the art online monitoring system for the waste beam in the rapid cycling synchrotron of the Japan Proton Accelerator Research Complex", *Phys. Rev. Spec. Top. Accel. Beams,* vol. 14, p. 119902, 2011. doi: 10.1103/PhysRevSTAB.14. 119902